Elsevier Editorial System(tm) for Journal of Theoretical Biology
Manuscript Draft

Manuscript Number: JTB-D-14-00610R1

Title: MODELING OF SENSING POTENCY OF CYTOSKELETAL SYSTEMS DECORATED WITH METABOLIC ENZYMES

Article Type: Regular Paper

Keywords: mathematical model; metabolism; microtubule; sensing

Corresponding Author: Prof. Judit Ovádi,

Corresponding Author's Institution: Institute of Enzymology, Research Centre for Natural Sciences, Hungarian Academy of Sciences

First Author: Judit Oláh

Order of Authors: Judit Oláh; Vic Norris; Judit Ovádi

Abstract: The highly dynamic cytoskeleton interacts with enzymes and other proteins that are involved in metabolic or signaling pathways. These interactions can influence the structural and functional characteristics of the partners at the microscopic level of individual proteins and polymers. In this work the functional consequences of such interactions have been studied at the macroscopic level in order to evaluate the integrative and regulatory roles of the metabolic pathways associated with the microtubule cytoskeleton. Here we present mathematical models of the interactions between a hypothetical metabolic pathway and microtubule assembly, and explore for the first time the functional consequences of these interactions in distinct situations. The models include kinetic constants of the individual steps and testable, relevant parameters which allow the quantification of the coupled processes at the microscopic and macroscopic levels. For example our kinetic model for the self-assembly of microtubules reproduces the alteration of the time-dependent turbidity caused by pyruvate kinase binding. Our data reveal the power of a mechanistic description of a filamentous system to explain how cells sense the state of metabolic and other pathways.

HIGHLIGHTS

The dynamic cytoskeleton interacts with proteins that are involved in metabolic or signaling pathways.

Mathematical models for the interactions of metabolic pathways and microtubule assembly are evaluated.

Functional consequences of these interactions are predicted in distinct situations.

A kinetic model with relevant parameters reproduces altered tubulin assembly caused by a glycolytic enzyme.

A mechanistic description allows the quantification of how cells sense the state of pathways.

MODELING OF SENSING POTENCY OF CYTOSKELETAL SYSTEMS DECORATED WITH METABOLIC ENZYMES

Judit Oláh[a], Vic Norris[b], Judit Ovádi[a§]

[a]Institute of Enzymology, Research Centre for Natural Sciences, Hungarian Academy of Sciences, H-1117, Budapest, Hungary; [b]Laboratory of Microbiology Signals and Microenvironment, EA 4312, Faculty of Science, University of Rouen, 76821, Mont Saint Aignan, France

[§]Address correspondence to: Judit Ovádi, Institute of Enzymology, Research Centre for Natural Sciences, Hungarian Academy of Sciences, Budapest, Magyar tudósok körútja 2., H-1117, Hungary, Tel. (36-1) 3826-714; E-mail: ovadi.judit@ttk.mta.hu

E-mail addresses:

J. Oláh: olah.judit@ttk.mta.hu;

VN: victor.norris@univ-rouen.fr;

J. Ovádi: ovadi.judit@ttk.mta.hu;

ABSTRACT

The highly dynamic cytoskeleton interacts with enzymes and other proteins that are involved in metabolic or signaling pathways. These interactions can influence the structural and functional characteristics of the partners at the microscopic level of individual proteins and polymers. In this work the functional consequences of such interactions have been studied at the macroscopic level in order to evaluate the integrative and regulatory roles of the metabolic pathways associated with the microtubule cytoskeleton. Here we present mathematical models of the interactions between a hypothetical metabolic pathway and microtubule assembly, and explore for the first time the functional consequences of these interactions in distinct situations. The models include kinetic constants of the individual steps and testable, relevant parameters which allow the quantification of the coupled processes at the microscopic and macroscopic levels. For example our kinetic model for the self-assembly of microtubules reproduces the alteration of the time-dependent turbidity caused by pyruvate kinase binding. Our data reveal the power of a mechanistic description of a filamentous system to explain how cells sense the state of metabolic and other pathways.

KEYWORDS

mathematical model, metabolism, microtubule, sensing

HIGHLIGHTS

The dynamic cytoskeleton interacts with proteins that are involved in metabolic or signaling pathways.

Mathematical models for the interactions of metabolic pathways and microtubule assembly are evaluated.

Functional consequences of these interactions are predicted in distinct situations.

A kinetic model with relevant parameters reproduces altered tubulin assembly caused by a glycolytic enzyme.

A mechanistic description allows the quantification of how cells sense the state of pathways.

1. INTRODUCTION

Metabolism in cells can be controlled according to the concept of cytoskeleton-driven modulation of enzymatic fluxes (Aon and Cortassa, 1997; Aon et al., 2000; and references therein) and/or metabolic channeling, which facilitates the intermediate transfer between the associated enzymes (stable or transient enzymatic complexes) (Ovádi and Srere, 2000, and references therein). There has been extensive theoretical and experimental analysis of the idea that the binding of metabolic enzymes to the cytoskeletal filaments affects their catalytic activity to cause significant alterations at microscopic and macroscopic levels; in addition, the sensitivity of these hetero-associations is modulated by factors such as the activity of the enzyme, its phosphorylation state, and interactions with other proteins (Aon and Cortessa, 2002, and references therein).

During the past decades an advanced level in the mathematical modeling of the main metabolic pathways has been achieved for different cell types (http://www.jjj.bio.vu.nl/cgi-bin/processModelSelection.py). One of these well- characterized pathways is glycolysis where the enzymes, in addition to their glycolytic activities, have structural functions that depend on their direct associations with the cytoskeletal networks (Aon and Cortassa, 2002; Cassimeris et al., 2012; Knull and Walsh, 1992; Ovádi et al., 2004; Sola-Penna et al., 2010). Although these models successfully characterize stationary and time-dependent metabolic states, many of them disregard the influence of an enzyme binding to the cytoskeleton. Relevant papers have been published in this field in the last decade by the Aon group (Aon et al., 1996; Aon and Cortassa, 1997; Aon et al., 2000; Aon and Cortessa, 2002; Cortassa et al., 1994). A mathematical model was formulated for the coupling of microtubular proteins to the glycolytic pathway and its branches: the Krebs cycle, ethanolic fermentation, and the pentose phosphate pathway in yeast (Aon and Cortessa, 2002). It was suggested that tubulin partitioning between dimer and polymer pools might regulate multiple steps in metabolism (Cassimeris et al., 2012), and that the rates of individual enzymatic steps and metabolite concentrations change with the polymeric status of microtubules throughout the metabolic network (Aon and Cortassa, 2002).

The multifunctional microtubule network, an integral part of the eukaryotic cytoskeleton along with actin and intermediate filaments, plays crucial roles in cell division, motility, intracellular trafficking

and the maintenance of cell shape and polarization (Conde and Caceres, 2009; de Forges et al., 2012). Cytoskeletal tubulin is also involved in the regulation of the voltage-dependent anion channel at the mitochondria-cytosol interface which ensures normal metabolite and energy exchange between mitochondria and cytoplasm through the permeability of the mitochondrial outer membrane (Rostovtseva and Bezrukov, 2012). The functionally important, reversible blockage of voltage-dependent anion channel by nanomolar to micromolar dimeric tubulin makes the mitochondrial outer membrane impermeable to ATP and other multi-charged anions (Rostovtseva et al., 2008).

Microtubules are known to interact with various glycolytic enzymes (Aon and Cortassa, 2002; Knull and Walsh, 1992; Sola-Penna et al., 2010). These transient interactions influence the structural and functional characteristics of both partners resulting in alterations in microtubule ultrastructure and enzyme activities (Ovádi et al., 2004). The binding of phosphofructokinase to microtubules results in the periodic cross-linking of microtubules and decreased enzyme activity due to the dissociation of the active tetrameric enzyme. The interaction between hexokinase and microtubules increases the activity of the enzyme without affecting the microtubule network, while the binding of pyruvate kinase impedes microtubule assembly without influencing the enzyme activity (Ovádi et al., 2004). While the interactions between glycolytic enzymes and cytoskeletal proteins have been intensively studied, much less is known about the consequences of the mutual interactions on the metabolic fluxes or the dynamics of the filamentous systems; one exception being the cardiomyocyte where microtubule stability was found to affect glycolysis during the early stages of hypoxia (Teng et al., 2010).

In the course of the microtubule assembly the head-to-tail association of tubulin heterodimers (composed of α and β tubulin monomers) into microtubules is coupled with multiple associations and various posttranslational modifications (Conde and Caceres, 2009; de Forges et al., 2012). Dynamic instability is a characteristic behavior of microtubules: an individual microtubule alternates between distinct phases of growth, pause and shrinkage, separated by rescue and catastrophe events, while the total amount of microtubules remains almost constant (Mitchison and Kirschner, 1984). This dynamic instability is central to the function of microtubules allowing them to reorganize rapidly, and to differentiate spatially and temporally in accordance with environmental signals and factors.

Reversible and irreversible nucleation-growth models, however, have been developed for tubulin polymerization based on Oosawa's classical model (Oosawa and Kasai, 1962; Morris et al., 2009; Flyvbjerg et al., 1996). The mathematical model for the one-dimensional polymerization dynamics of rod-like polymers such as actin or tubulin proposed by Edelstein-Keshet and Ermentrout (Edelstein-Keshet and Ermentrout, 1998, 2000) can explain satisfactorily the length distribution of polymers when, following the initial nucleation, the reversible polymerization of subunits and the depolymerization of polymers are taken into account.

All these data led us to propose an integrative and regulatory role for microtubules in the metabolism of cells (Norris et al., 2012). In this hypothesis, the cytoskeleton senses and integrates the metabolic activity of the cells so as to meet the challenge of generating a single phenotype that must be coherent with various internal and external conditions (Ovádi and Norris, 2014). In the work presented here, we use mathematical models to predict the dynamics of tubulin polymerization coupled with kinetics of metabolite concentrations as a function of time in conditions in which metabolic enzymes bind to distinct polymers of the tubulin units. The result of this modeling is a quantitative description of the relationship between microtubule dynamics and kinetics of metabolite concentrations as a function of time which validates the hypothesis that the enzyme-decorated cytoskeletal microtubular network possesses a powerful sensing potency to transduce the information about the metabolic state of the cell into cytoskeletal dynamics.

2. MATERIALS AND METHODS

All the numerical simulations were performed with Mathematica for Students (version 4.1.1.0) software package (Wolfram Research; http://www.wolfram.com).

3. RESULTS

A mathematical model has been developed that couples the self-assembly of tubulin subunits into polymers of different lengths (leading to the formation of microtubules) with the association with these polymers of an enzyme involved in a metabolic pathway. This model, $MODEL_{coupled}$, includes kinetic

parameters characteristic of the assembly/disassembly of polymers and the enzyme binding to tubulin species; the model can predict the consequences of the hetero-association of the tubulin species and the enzyme on microtubule dynamics and kinetics of metabolite concentrations as a function of time. In addition, this model is extended to quantify the possible effect of a modulator on the coupled processes at the macroscopic level.

3.1 Tubulin polymerization at microscopic and macroscopic levels

The initial premises for the modeling of microtubule assembly/disassembly ($MODEL_{assembly}$) are the following: i) microtubule assembly starts with nucleation that originates from the association of two subunits; ii) nucleation is followed by the reversible polymerization/depolymerization of tubulin species by association/dissociation of subunits to/from the polymers; iii) the length of polymers considered as microtubules is restricted; iv) the rate constants of the assembly/disassembly, k_{on} and k_{off}, are independent of the length of the polymer except that of the nucleation (k_{init}) as well as that of the depolymerization of the maximum length polymer (k_c); v) the 3D tube structure of microtubules is disregarded and they are considered as rod-like polymers. Accordingly, the time-dependent concentrations of the tubulin species can be calculated as described by equ.1 (Edelstein-Keshet and Ermentrout, 1998):

$$d\left[T_j\right]/dt = k_{off}\left[T_{j+1}\right] - k_{off}\left[T_j\right] - k_{on}\left[T_j\right]\left[T_1\right] + k_{on}\left[T_{j-1}\right]\left[T_1\right] \qquad \text{equ.1}$$

where $[T_j]$ represents the actual concentration of a given polymer consisting of j subunits which is produced by the depolymerization of $[T_{j+1}]$ as well as the polymerization of $[T_{j-1}]$, and consumed because of its depolymerization into $[T_{j-1}]$ and polymerization into $[T_{j+1}]$.

By numerically solving the set of differential equations (see Supplementary data), the time-dependent tubulin polymerization/depolymerization processes can be determined at the microscopic level. At the macroscopic level, the tubulin assembly can be monitored by the well-known turbidity measurements. Tubulin polymers with a length of 350 nm or longer are not transparent, and thus produce a turbidity which is suitable for spectrophotometric detection at 350 nm. Microtubules 1 μm long are built up from about 1600

subunits (Edelstein-Keshet and Ermentrout, 2000), therefore polymers producing turbidity (i.e., polymers longer than 350 nm) contain 550 or more subunits (equ 2).

$$\sum_{j=550}^{800} j\left[T_j\right] = \text{Turbidity} \qquad \text{equ.2}$$

The Edelstein-Keshet and Ermentrout model does not exploit the light-scattering features of polymers which allow one to follow directly the polymerization by turbidimetry; in contrast, the $MODEL_{assembly}$ defines the number of subunits in microtubules producing turbidity. This is an important issue because it makes it possible to convert microscopic parameters into macroscopic ones and to correlate the computed polymerization of tubulin species with in vitro experimental data.

The $MODEL_{assembly}$ (Fig. 1, Table S1, supplementary data) describes the three characteristic phases of tubulin assembly: the lag phase corresponding to nucleation; the growth phase when tubulin subunits are added to the polymers causing elongation and when the number of microtubules increases; the equilibrium phase when polymerization and depolymerization proceed at equal rates as illustrated at microscopic (Fig. 1A) and macroscopic (Fig. 1B) levels. According to $MODEL_{assembly}$ (Fig. 1), only a small amount of the tubulin subunits polymerized into visible microtubules with lengths between 350 and 500 nm (corresponding to 550-800 subunits). The 10 μM initial tubulin subunit concentration is typical for in vitro tubulin polymerization experiments which are usually in the 5-20 μM concentration range and are very sensitive to alterations.

Below the critical concentration no polymerization occurs. Indeed, according to our model, at an initial subunit concentration of 8 μM the tubulin polymerization is significantly reduced (to about 10%), while at 15 μM it is significantly increased (Fig. 1B). The rate constants, k_{on} and k_{off}, we used, were determined experimentally from in vitro assays of tubulin polymerization in quasi-physiological conditions (Walker et al., 1988). The presence of microtubule-associated proteins or different polymerization-enhancing drugs such as paclitaxel significantly influences the rate constants and the polymerization dynamics (Burns, 1991).

3.2 Enzyme catalyzed reactions at microscopic and macroscopic levels

The $MODEL_{metabolism}$ describes a simple metabolic pathway where the consecutive reactions are catalyzed by three functionally related enzymes. All reactions are considered reversible (see Supplementary data), and the time-dependent concentrations of the substrate, intermediates and the final product are shown both for a closed and an open system (Fig. 2). In the closed system there is no influx or efflux for the metabolites, and the initial substrate concentration is one order of magnitude higher then the Michaelis-Menten constants of enzymes (Fig. 2A, Table S2 and S3, Supplementary data). In the case of the open system, the substrate concentration was kept constant corresponding to equilibrated influx of the substrate, and a constant efflux rate constant with first-order kinetics was assumed for product transport, which ensured steady-state (Fig. 2B, Table S2 and S3, Supplementary data).

The $MODEL_{metabolism}$ describes the time-dependent concentrations of all metabolites, S, I_1, I_2 and P in different conditions assuming k_{cat} and K_M values for the individual enzyme reactions with reversible Michaelis-Menten kinetics (equ. 3) (Table S2, Supplementary data).

$$v_2 = (k_{cat2}[E_2] / K_{M2}) * ([I_1] - [I_2] / K_{e2}) / (1 + [I_1] / K_{M2} + [I_2] / K_{M22}) \qquad \text{equ.3}$$

3.3 Evaluation of the sensing potency of the microtubule system: coupling of tubulin assembly/disassembly to metabolism

The sensing potency of the cytoskeleton is the capacity of the enzyme-decorated cytoskeleton to transduce the information about the metabolic state of the cell into cytoskeletal dynamics (Norris et al., 2013). The $MODEL_{coupled}$ describes the coupling of the two processes at the system level – tubulin assembly/disassembly and metabolism – due to the binding of a single enzyme of the pathway, E_2, to tubulin species. This heteroassociation has functional consequences on both processes. Let us assume that both the polymerization of tubulin and the activity of E_2 are inhibited: the rate constant of the polymerization (k^*_{on}) and the activity of the E_2-T_j heterocomplexes, Q_j ($k_{cat2\text{-}Qj}$) are reduced by 50%. Due to this new situation, additional parameters have to be defined such as k^*_{on}, k^*_{off} characteristic of the polymerization of E_2-bound tubulin species, $k_{on\text{-}Qj}$ and $k_{off\text{-}Qj}$ characteristic of the formation of Q_j species as well as $k_{cat2\text{-}Qj}$ representing the

enzyme activity of Q_j (Table S1 and S2, Supplementary data). The scheme of $MODEL_{coupled}$ is shown (Fig 3A).

The time courses of the coupled processes with the parameter sets presented in Table S1 and S2 are computed assuming that E_2 binds to tubulin species with the same affinity independently of their polymerization states (equ. 4) (see Supplementary data). These time courses show both the sensing potency of the microtubule system to varying the kinetic parameters (Fig. 3B, Fig. S1 and S3A) and the accompanying changes in the time-dependent metabolic concentrations (Fig. 3C and 3D, Fig. S2 and S3B and C, Table S3).

$$d[E_2]/dt = -(\sum_{j=1}^{800} k_{on-Qj}[T_j])[E_2] + (\sum_{j=1}^{800} k_{off-Qj}[Q_j]) \qquad \text{equ.4}$$

The dynamics of the microtubule system can be drastically altered by heteroassociations between tubulin species and metabolic enzymes that, in fact, is the case for the tubulin polymerization system. This means that the dynamics of the microtubule system could transduce information about metabolic activity provided that this information is in the form of altered affinities of enzymes for tubulin species, as in the metabolic sensing model.

The analysis of the time courses of the coupled microtubule assembly and a hypothetical metabolic pathway evaluated in both open and closed systems at distinct kinetic parameters allows one to draw some conclusions by comparing with the time courses of the uncoupled ones (Fig. 3, Table S3). i) The *coupling effect* manifests itself in the $Model_{coupled}$ as compared to the $Model_{assembly}$ and $Model_{metabolism}$ and is maintained in the case of both the open and the closed systems; however, the analysis of the open system, where each metabolite, S, I_1, I_2 and P, is in steady state, makes it possible to characterize the coupling effect quantitatively. Accordingly, the coupling effect led to the result that while $[I_1]$ increased by about 50-70%, $[I_2]$ and [P] decreased by about 40-60% and 30-40%, respectively, which apparently was not influenced by changing the influx and efflux rates of the [S] and [P], respectively. ii) The coupling effect was very clear for the tubulin assembly process; this effect is, however, independent whether the system is open or closed (cf. Fig. 3B). It has to be emphasized therefore that the inhibition of a single enzyme of a metabolite pathway due

to its binding to tubulin polymers significantly increases the steady-state concentration of an intermediate (the substrate of the inhibited E_2) while the concentrations of the other metabolites were reduced so allowing regulatory effects when the pathway lies at a metabolic cross-roads. The time courses also show that heteroassociations between tubulin species and metabolic enzymes, assuming an altered $k_{cat2\text{-}Qj}$ of E_2 catalyzed reaction, can significantly affect the time-dependent metabolite concentrations (Fig. 3C and 3D, Fig. S3B and C, Table S3). This raises the question of whether a two-way (mutual) relationship based on heteroassociation affecting between microtubule dynamics and metabolic activity creates basins of attraction so that the system converges onto stable combinations of microtubule dynamics and metabolic activity with particular values as long as the heteroassociation of E_2 to tubulin species is not modulated. That said, a change in $k_{off\text{-}Qj}$ affecting the heteroassociation between E_2 and the tubulin species is only slightly reflected in the metabolism at the macroscopic level, while the tubulin assembly/disassembly shows high sensitivity (Fig. S3A, B and C). This finding indicates that there is situation in which the heteroassociation of the constituents of the interrelated processes produces distinct effects (sensitivity) on the individual pathways that is determined by the parameters of the individual steps.

3.4 Modulation of the sensing potency of the microtubule system

Now we consider a physiologically relevant situation when intracellular factors or modulators, ranging from small metabolites to large macromolecules, perturb the binding of metabolic enzymes to tubulin species; in this situation, the cytoskeleton can play an important role in sensing the metabolic state of the cell (Norris et al., 2013). The extra, initial premise to describe this effect of a modulator by $MODEL_{modulator}$ as compared to $MODEL_{coupled}$ is that the modulator, M, inhibits the E_2 binding to tubulin species by forming an E_2-M complex, and thus reduces the concentration of the T_j-E_2 (Q_j) complex (Fig. 3A, Fig. S4, Table S1, S2 and S3, Supplementary data). Modeling this complex phenomenon makes it possible to simulate the effect of both small and macromolecular modulators on the interrelated metabolism and tubulin polymerization. The extent of the modulating effect depends on the ratio of dissociation constants of the Q_j and E_2-M complexes (K_T and K_M, respectively) (equ. 5-6) as well as the concentrations of the components involved in the heterogeneous associations. The results of the $MODEL_{modulator}$ scheme and the extended equation to describe the association of E_2 (equ. 7) are shown (Fig. 3).

$$K_T = [E_2][T_j]/[Q_j] = k_{off-Qj} / k_{on-Qj} \quad \text{equ.5}$$

$$K_M = [E_2][M]/[E_2 - M] = k_{off-M} / k_{on-M} \quad \text{equ.6}$$

$$d[E_2]/dt = -(\sum_{j=1}^{800} k_{on-Qj}[T_j])[E_2] + (\sum_{j=1}^{800} k_{off-Qj}[Q_j]) - k_{on-M}[E_2][M] + k_{off-M}[E_2 - M] \quad \text{equ.7}$$

The time courses computed using $MODEL_{modulator}$ show that the modulator, M, can affect the sensing potency of the microtubule system, and that increasing the modulator concentration significantly increases both the tubulin assembly and the time-dependent product concentration by counteracting the inhibitory effect of E_2 (Fig. S4, Table S3). This observation is of great importance and shows not only that the inhibitory potency of a metabolic enzyme, but also that, in principle, the enzyme association could be transduced into an altered polymerization of microtubules.

3.5 Application of the analysis for an experimental system

Previously, we have shown the inhibitory effect of pyruvate kinase (PK) on tubulin polymerization (turbidity) and the modulating role of phosphoenolpyruvate (PEP) on the PK-tubulin/microtubule interactions (Kovacs et al., 2003). PEP is a glycolytic intermediary and the substrate of PK. In this system, tubulin, PK and PEP were present at constant concentrations (10, 2 and 100 μM, respectively), the dissociation constant characteristic for the PK-tubulin interaction (K_D = 0.042 μM) was determined experimentally by surface plasmon resonance, and the turbidity of the tubulin solution was determined in the absence and presence of PK and/or PEP. However, tubulin polymerization was induced by the addition of paclitaxel in this system, which significantly modifies the polymerization dynamics, decreases the critical concentration, and the soluble tubulin becomes negligible in the equilibrium phase (Burns, 1991; Vértessy et al., 1997). Therefore the following parameters presented in Table S4 were used for modeling the experimentally measured data (Fig. 4).

The model qualitatively describes the inhibitory effect of PK on tubulin polymerization, and the counteracting effect of PEP. Assuming that all 10 μM tubulin is in polymerized form in the equilibrium phase which has been confirmed by pelleting experiments (Kovacs et al., 2003), on the basis of the following relationship that 1 unit of absorbance at 350 nm was estimated as produced by assembled tubulin of 44 μM (Burns, 1991), the 0.5 absorbance produced by 10 μM tubulin in our turbidity measurement is reasonable.

4. CONCLUSION

The objective of the studies presented in this paper was to provide a quantitative description of the cytoskeletal integrative sensor hypothesis presented previously (Norris et al., 2013). According to this hypothesis, the cytoskeleton senses and integrates the general metabolic activity of the cell which depends on the binding to the cytoskeleton of enzymes and, depending on the nature of the enzyme; this binding may occur if the enzyme is either active or inactive but not both.

In this work, physiologically plausible mathematical models were developed which make it possible to establish the effect of the coupling between two biological processes, metabolism and cytoskeletal dynamics. These models allowed us to quantitatively characterize the sensing potency of these systems. In fact, it has been reported that tubulin partitioning between dimer and polymer pools may regulate multiple steps in metabolism (Cassimeris et al., 2012), and that the rates of individual enzymatic steps and metabolite concentrations vary with the polymeric status of microtubules throughout the metabolic network (Aon and Cortassa, 2002). These authors built experiment-based mathematical models that showed that the glycolytic flux increases or decreases with increased or decreased levels of polymerized tubulin, respectively due to the change of the activity of the individual enzymes with the polymeric status of tubulin. In our cases the reversible assembly and disassembly process of the tubulin/microtubule system is described by kinetic parameters and criteria which make the process physiologically relevant even if the formation of linear chains with distinct lengths and not 3D tubes are considered (it should be added that the mechanism of the formation of the tubes has not been unambiguously established). Our model systems are able to simulate the dynamics of cytoskeleton and metabolism at the macroscopic level in the cases of defined enzymatic

reactions regulated by the concentration of tubulin polymers, the local concentrations of substrates, enzymes, and modulators as well as the polymeric status of the tubulin polymers. Evaluation of the models showed that they provide simplified but realistic description of the coupled dynamic processes at the macroscopic level since the experimental data could be reproduced by modeling the binding of metabolite-modulated glycolytic enzymes to tubulin polymers (cf. Fig. 4). Finally, it has to be emphasized that the model, $Model_{coupled,}$ presented here can be extended to include changes to the number and nature of the hetero-associations, different numerical values for the parameters, and even new parameters needed to study the mechanisms characteristic of individual steps of the polymerization and enzyme reactions (e.g. formation of 3D polymers).

5. LIST OF ABBREVIATIONS USED

phosphoenolpyruvate, PEP; pyruvate kinase, PK.

6. COMPETING INTERESTS

The authors declare no conflict of interest.

7. ACKNOWLEDGEMENTS

Funding: This work was supported by the European Commission [(DCI ALA/19.09.01/10/21526/ 245-297/ALFA 111(2010)29], European Concerted Research Action [COST Action TD0905 and TD1304]; Hungarian National Scientific Research Fund Grants OTKA [T-101039] and Richter Gedeon Nyrt [4700147899] to J. Ovádi.

8. REFERENCES

Aon, M.A. and Cortassa, S. (2002) Coherent and robust modulation of a metabolic network by cytoskeletal organization and dynamics. Biophys. Chem., 97, 213-231.

Aon, M.A., Cortassa, S., Gomez Casati, D.F. and Iglesias, A.A. (2000) Effects of stress on cellular infrastructure and metabolic organization in plant cells., Int. Rev. Cytol., 194, 239-273.

Aon, M.A. and Cortassa, S. (1997) Dynamic Biological Organization: Fundamentals as Applied to Cellular Systems., Chapmanand Hall, London.

Aon, M.A., Cáceres, A. and Cortassa, S. (1996) Heterogeneous distribution and organization of cytoskeletal proteins drive differential modulation of metabolic fluxes., J. Cell. Biochem., 60, 271-278.

Burns, R.G. (1991) Assembly of chick brain MAP2-tubulin microtubule protein. Characterization of the protein and the MAP2-dependent addition of tubulin dimers., Biochem. J., 277 (Pt 1), 231-238.

Cassimeris, L., Silva, V.C., Miller, E., Ton, Q., Molnar, C. and Fong, J. (2012) Fueled by microtubules: does tubulin dimer/polymer partitioning regulate intracellular metabolism?, Cytoskeleton (Hoboken), 69, 133-143.

Conde, C. and Caceres, A. (2009) Microtubule assembly, organization and dynamics in axons and dendrites. Nat. Rev. Neurosci., 10, 319-332.

Cortassa, S., Cáceres, A. and Aon, M.A. (1994) Microtubular protein in its polymerized or nonpolymerized states differentially modulates in vitro and intracellular fluxes catalyzed by enzymes of carbon metabolism., J. Cell. Biochem., 55, 120-132.

de Forges, H., Bouissou, A. and Perez, F. (2012) Interplay between microtubule dynamics and intracellular organization. Int. J. Biochem. Cell. Biol., 44, 266-274.

Edelstein-Keshet, L. and Ermentrout, G.B. (1998) Models for the length distributions of actin filaments: I. Simple polymerization and fragmentation. Bull. Math. Biol., 60, 449-475.

Edelstein-Keshet, L. and Ermentrout, G.B. (2000) Models for spatial polymerization dynamics of rod-like polymers. J. Math. Biol. 40, 64-96.

Flyvbjerg, H., Jobs, E. and Leibler, S. (1996) Kinetics of self-assembling microtubules: an "inverse problem" in biochemistry. Proc. Natl. Acad. Sci. U S A, 93, 5975-5979.

Knull, H.R. and Walsh, J.L. (1992) Association of glycolytic enzymes with the cytoskeleton. Curr. Top. Cell. Regul., 33, 15-30.

Kovács, J., Lőw, P., Pácz, A., Horváth, I., Oláh, J. and Ovádi, J. (2003) Phosphoenolpyruvate-dependent tubulin-pyruvate kinase interaction at different organizational levels. J. Biol. Chem., 278, 7126-7130.

Mitchison, T. and Kirschner, M. (1984) Dynamic instability of microtubule growth. Nature, 312, 237-242.

Morris, A.M., Watzky, M.A. and Finke, R.G. (2009) Protein aggregation kinetics, mechanism, and curve-fitting: a review of the literature. Biochim. Biophys. Acta, 1794, 375-397.

Norris, V., Amar, P., Legent, G., Ripoll, C., Thellier, M. and Ovádi, J. (2013) Sensor potency of the moonlighting enzyme-decorated cytoskeleton: the cytoskeleton as a metabolic sensor. BMC Biochem., 14, 3.

Oosawa, F. and Kasai, M. (1962) A theory of linear and helical aggregations of macromolecules. J. Mol. Biol., 4, 10-21.

Ovádi, J., Orosz, F. and Hollán, S. (2004) Functional aspects of cellular microcompartmentation in the development of neurodegeneration: mutation in-duced aberrant protein-protein associations. Mol. Cell. Biochem., 256-257, 83-93.

Ovádi, J. and Norris, V. (2014) Moonlighting Function of the Tubulin Cytoskeleton: Macromolecular Architectures in the Cytoplasm. in: Aon, M. A., Saks, V. and Schlattner, U. (Eds.), Systems Biology of Metabolic and Signaling Networks. Energy, Mass and Information Transfer., Springer, 165-178.

Ovádi, J. and Srere, P.A. (2000) Macromolecular compartmentation and channeling., Int. Rev. Cytol., 192, 255-280.

Rostovtseva, T.K. and Bezrukov, S.M. (2012) VDAC inhibition by tubulin and its physiological implications., Biochim. Biophys. Acta, 1818, 1526-1535.

Rostovtseva, T.K., Sheldon, K.L., Hassanzadeh, E., Monge, C., Saks, V., Bezrukov, S.M. and Sackett, D.L. (2008) Tubulin binding blocks mitochondrial voltage-dependent anion channel and regulates respiration., Proc. Natl. Acad. Sci. U S A, 105, 18746-1851.

Sola-Penna, M., Da Silva, D., Coelho, W.S., Marinho-Carvalho, M.M. and Zancan, P. (2010) Regulation of mammalian muscle type 6-phosphofructo-1-kinase and its implication for the control of the metabolism. IUBMB Life, 62, 791-796.

Teng, M., Dang, Y.M., Zhang, J.P., Zhang, Q., Fang, Y.D., Ren, J. and Huang, Y.S. (2010) Microtubular stability affects cardiomyocyte glycolysis by HIF-1alpha expression and endonuclear aggregation during early stages of hypoxia. Am. J. Physiol. Heart Circ. Physiol., 298, H1919-1931.

Vértessy, B.G., Kovács, J., Lőw, P., Lehotzky, A., Molnár, A., Orosz, F. and Ovádi, J. (1997) Characterization of microtubule-phosphofructokinase complex: specific effects of MgATP and vinblastine. Biochemistry, 36, 2051-2062.

Walker, R.A., O'Brien, E.T., Pryer, N.K., Soboeiro, M.F., Voter, W.A., Erickson, H.P. and Salmon, E.D. (1988) Dynamic instability of individual microtubules ana-lyzed by video light microscopy: rate constants and transition frequencies. J. Cell. Biol., 107, 1437-1448.

9. FIGURE LEGENDS

Figure 1. Time-dependent tubulin polymerization at microscopic (A) and macroscopic (B) levels. MODEL$_{assembly}$. (A) Tubulin subunits (T_1) (bold line), polymer T_{400} (thin line), polymer T_{500} (dashed line) and microtubules consisting of 600 subunits (T_{600}) (dotted line) at 10 μM total tubulin concentration. (B) Turbidity (tubulin polymers contain 550 or more subunits) at 8 μM (dashed line), 10 μM (thin line) and 15 μM (dotted line) total tubulin concentration.

Figure 2. Time-dependent changes of metabolite concentration (MODEL$_{metabolism}$) in the case of closed (A) and open (B) systems. Substrate S (bold line), intermediates I_1 and I_2 (dashed and dotted line) and the product P (thin line). v_1, v_2 and v_3 are the rates of the individual reactions catalyzed by E_1, E_2 and E_3, respectively. S[0]=1000 μM and S[0]=100 μM for the closed and open systems, respectively.

Figure 3. Tubulin polymerization uncoupled/coupled with metabolism with or without modulator in the case of the closed and the open systems. (A) Reaction scheme for the possible models. (B) Time-dependent change of turbidity at 10 μM total tubulin concentration. Time-dependent change of the product P at S[0]=1000 μM and S[0]=100 μM in the closed (C) and open (D) systems, respectively. MODEL$_{assembly}$ or MODEL$_{metabolism}$ as control (solid line), MODEL$_{coupled}$ (dashed line), MODEL$_{modulator}$ (dotted line) (B-D).

Figure 4. Paclitaxel-induced tubulin polymerization (solid line) in the presence of PK without (dashed line) or with (dotted line) PEP. (A) Turbidity measured experimentally at 350 nm (Kovacs et al., 2003). (B) Alterations of turbidity according to the model. $k_{on\text{-}PEP}$ = 0.00007 $\mu M^{-1}sec^{-1}$ (dash-dot-dotted line).

4. Figure 1

Click here to download high resolution image

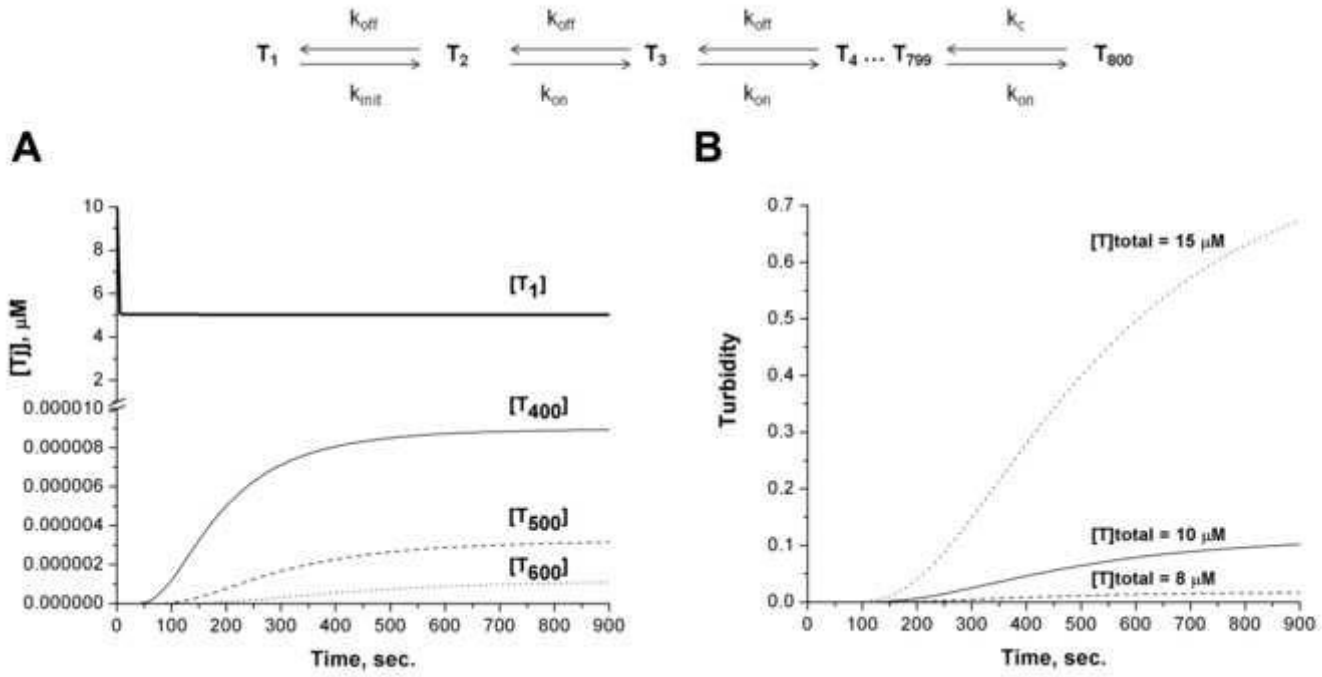

4. Figure 2

Click here to download high resolution image

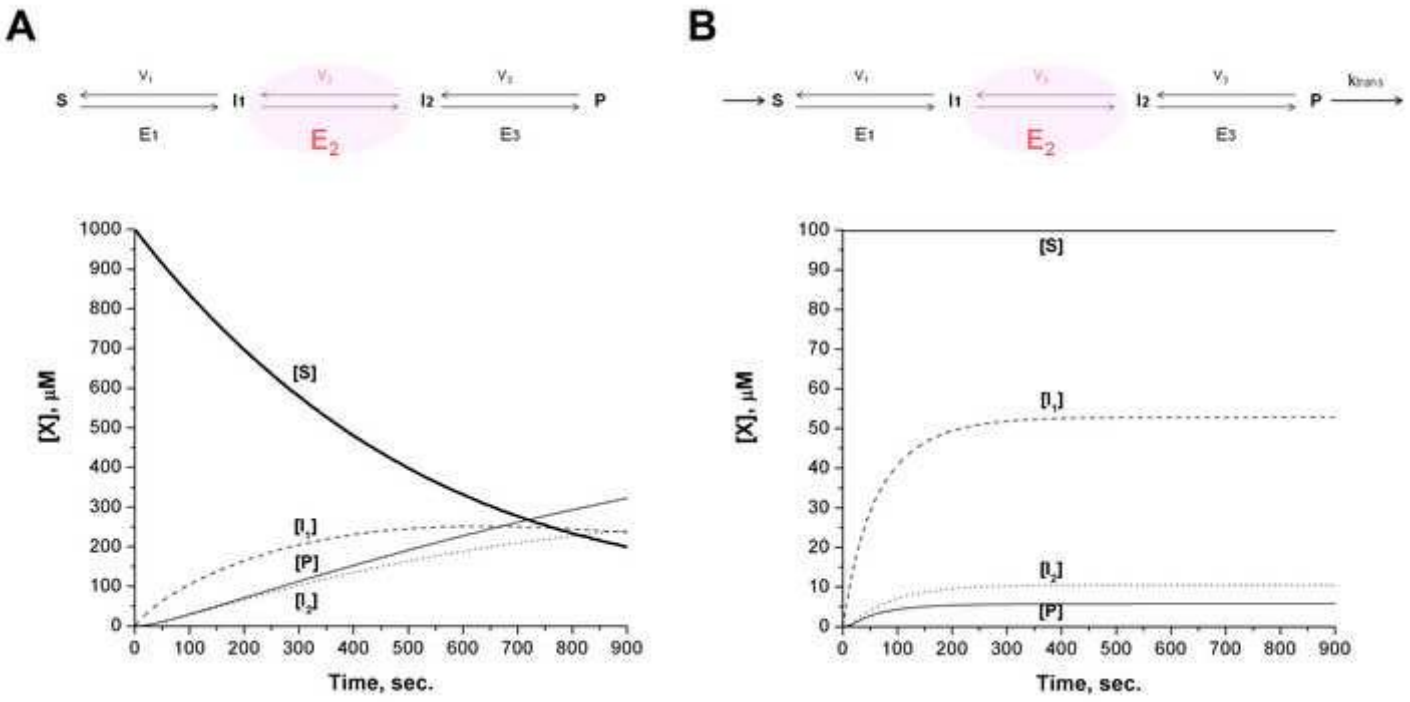

4. Figure 3
Click here to download high resolution image

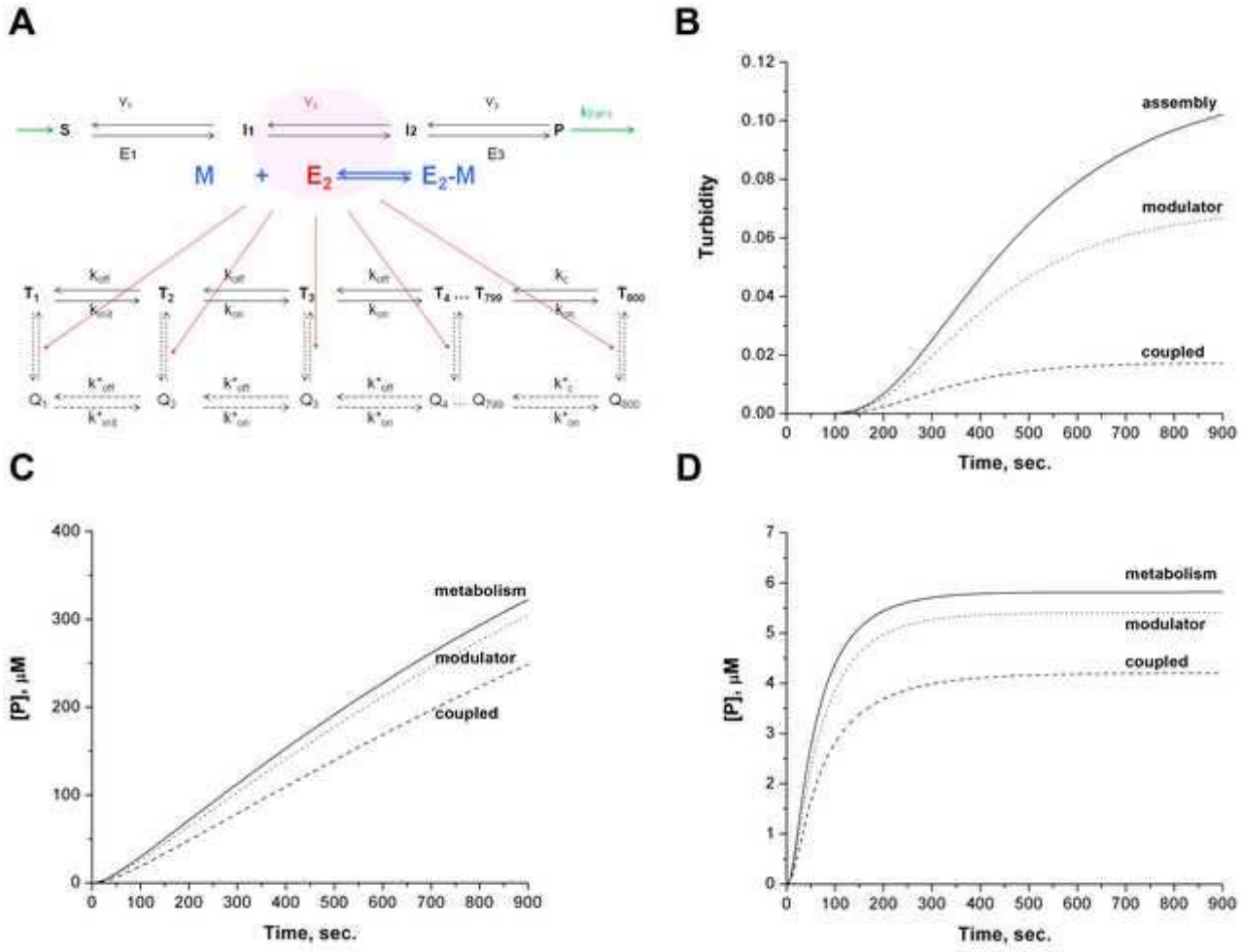

4. Figure 4
Click here to download high resolution image

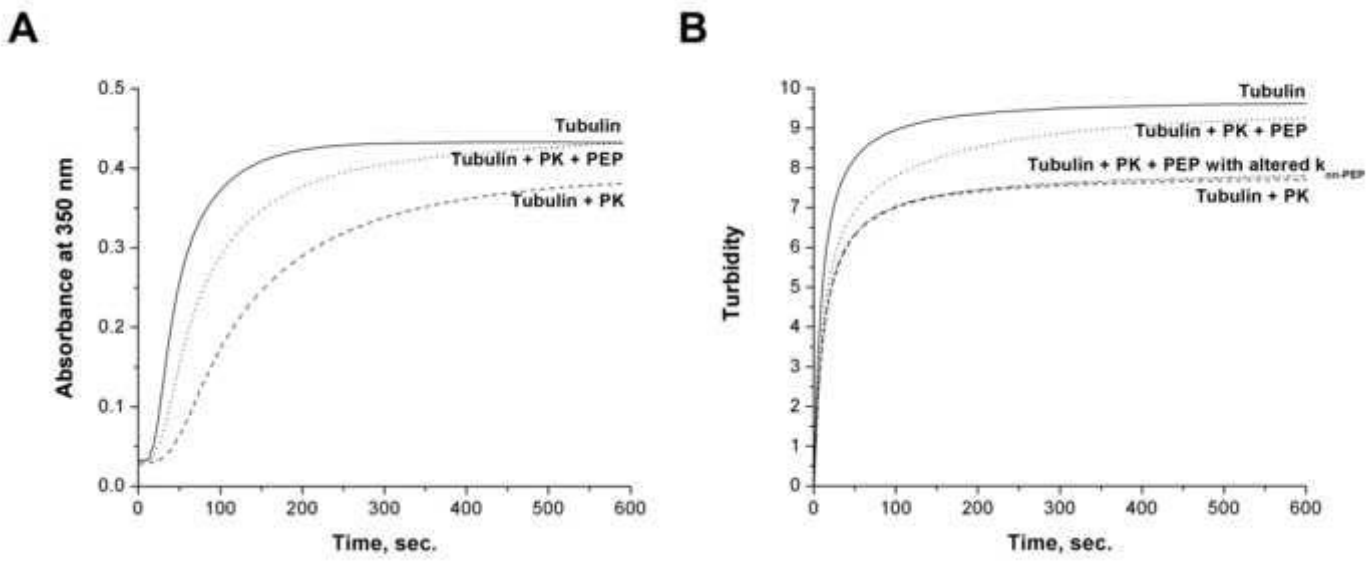

6. Supplementary Material for on-line publication only

Click here to download 6. Supplementary Material for on-line publication only: TABLE_S1.docx

6. Supplementary Material for on-line publication only

Click here to download 6. Supplementary Material for on-line publication only: TABLE_S2.docx

6. Supplementary Material for on-line publication only

Click here to download 6. Supplementary Material for on-line publication only: TABLE_S3.docx

6. Supplementary Material for on-line publication only

Click here to download 6. Supplementary Material for on-line publication only: TABLE_S4.docx

6. Supplementary Material for on-line publication only

Click here to download 6. Supplementary Material for on-line publication only: Supp FigureLegend_S1_S2_S3_S4.docx

6. Supplementary Material for on-line publication only

Click here to download 6. Supplementary Material for on-line publication only: Figure_Supp_1_nolayers_140905.tif

6. Supplementary Material for on-line publication only

Click here to download 6. Supplementary Material for on-line publication only: Figure_Supp_2_nolayers_140905.tif

6. Supplementary Material for on-line publication only

Click here to download 6. Supplementary Material for on-line publication only: Figure_Supp_3_nolayers_140905.tif

6. Supplementary Material for on-line publication only

Click here to download 6. Supplementary Material for on-line publication only: Figure_Supp_4_nolayers_140905.tif

6. Supplementary Material for on-line publication only

Click here to download 6. Supplementary Material for on-line publication only: Supplementary_Data.docx